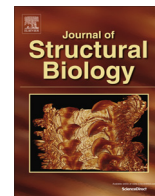




Contents lists available at ScienceDirect

Journal of Structural Biology

journal homepage: www.elsevier.com/locate/yjsbi

Cellular electron cryo tomography and *in situ* sub-volume averaging reveal the context of microtubule-based processes

Michael Grange, Daven Vasishtan, Kay Grünewald*

Oxford Particle Imaging Centre, Division of Structural Biology, Wellcome Trust Centre for Human Genetics, University of Oxford, Oxford, OX3 7BN, United Kingdom

ARTICLE INFO

Article history:

Received 7 April 2016

Received in revised form 27 June 2016

Accepted 28 June 2016

Available online xxxxx

Keywords:

Electron cryo-tomography

Cellular architecture

Sub-volume averaging

Microtubules

Cytoskeleton

Dynein

Adenovirus

Electron cryo-microscopy

Virus trafficking

Viral entry

Retrograde transport

Endocytosis

in situ structure determination

ABSTRACT

Electron cryo-tomography (cryoET) is currently the only technique that allows the direct observation of proteins in their native cellular environment. Sub-volume averaging of electron tomograms offers a route to increase the signal-to-noise of repetitive biological structures, such as improving the information content and interpretability of tomograms. We discuss the potential for sub-volume averaging in highlighting and investigating specific processes *in situ*, focusing on microtubule structure and viral infection. We show that (i) *in situ* sub-volume averaging from single tomograms can guide and complement segmentation of biological features, (ii) the *in situ* determination of the structure of individual viruses is possible as they infect a cell, and (iii) novel, transient processes can be imaged with high levels of detail.

© 2016 Published by Elsevier Inc.

1. Introduction

Electron cryo tomography (cryoET) is a technique used to reconstruct 3-dimensional structures of biological samples in their native, frozen hydrated state. By taking a tilt series of images of vitrified cells (or other relevant specimens) in an electron microscope it becomes possible to visualize unique pleomorphic events, structures with short-lived and transient states, and large macromolecular organisations (e.g. lattices) that would be otherwise very difficult to reconstitute *in vitro* (Asano et al., 2015; Brandt et al., 2010; Hagen et al., 2015; Schur et al., 2015; Zeev-Ben-Mordehai et al., 2016). Furthermore, repetitive or frequently occurring molecular structures within these pleomorphic objects can be averaged together to create higher resolution maps, a technique generally referred to as sub-tomogram averaging.

Recent technical developments in electron cryo microscopy (cryoEM) have resulted in the ability to image and collect data of vitrified specimens with unprecedented signal-to-noise ratios,

allowing the analysis of biological structures and features at a much higher level of detail than previously attainable. These developments include better zero-loss energy filters and direct electron detectors, both of which have vastly improved the quality of tomographic data acquisition (Koster et al., 1997; Li et al., 2013; McMullan et al., 2014), and led to the high-resolution determination of novel macromolecular complexes and viruses, as well as the structural determination of pleomorphic complexes and the *in situ* architecture of cells (Asano et al., 2015; Bartesaghi et al., 2015; Fukuda et al., 2015; Mahamid et al., 2016; Matthies et al., 2016; Schur et al., 2015; Sirohi et al., 2016; Zeev-Ben-Mordehai et al., 2016).

This move to analyze native cellular structures *in situ* has come concomitantly with a push towards the development of technologies such as Zernike phase plates, and more recently Volta phase plates (VPP) (Danev et al., 2014; Murata et al., 2010), that improve the image contrast. These improvements further include specimen thinning methods mitigating some of the detrimental impact of thick specimens – cells are typically too thick to image through standard methods, as the penetration limit of electrons through a frozen-hydrated specimen at 300 keV is around 1 μm

* Corresponding author.

E-mail address: kay@strubi.ox.ac.uk (K. Grünewald).

(Baumeister, 2002) – and allow us to use cryoET to image processes anywhere in the interior of cells (Al-Amoudi et al., 2004; Rigort et al., 2012). However, such techniques are still limited and challenging to implement technically.

Alternatively, it is also possible to avoid this thickness limit by focusing attention to the cell periphery. These areas of the cell are generally thin enough to be successfully imaged, and are accessible directly after plunge freezing such offering a much more widely and routinely used route of specimen preparation for many structural and cell biologists. Understanding the cell periphery is crucial to comprehending many biological mechanisms. These include, but are not limited to, cell signaling, translation, exocytosis, endocytosis, pathogen entry and egress and cytoskeletal organization and trafficking (Brandt et al., 2010; Cyrklaff et al., 2007; Dodonova et al., 2015; Ibiricu et al., 2011).

In this work, we assess what can be achieved by targeting the cellular periphery of whole intact non-thinned cells in individual tomograms, particularly through sub-volume averaging and the localization of rare events (Fig. 1A). We discuss the opportunities that novel developments offer to structural cell biologists when using direct electron detectors, especially when combined with an energy filter. Our assessment shows that the majority of information to determine usable and contextual structures is contained within the tomogram. As examples we reveal a range of regular structures that are discernible throughout the tomograms and assess their roles and interaction in the course of viral entry.

2. Materials and methods

2.1. Cell culture and plunge freezing

U87MG cells and U2OS cells were seeded and grown on poly-L-lysine-coated gold mesh carbon coated holey carbon grids (Electron microscopy sciences) in Dulbecco's modified eagle medium (DMEM) (Gibco) supplemented with 10% fetal bovine serum. The cells were grown to approximately 60–80% confluency, or until 1–2 cells per grid square. The grids were supported in 2×9-well μ -slide co-culture dishes (Ibidi). Adenovirus particles were cultured and isolated as has been described previously (Wodrich et al., 2010). For infection of U2OS cells with adenovirus, 4 μ l of adenovirus was mixed in 200 μ l of DMEM. 50 μ l was applied to each grid and incubated with the cells for 10–20mins before plunge freezing. Grids were plunge frozen in an ethane/propane mix, cooled to liquid nitrogen temperature using a manual blotting apparatus, blotted from the backside of the grid for between 2 and 4 s.

2.2. Electron microscopy

Tomograms were acquired using a Tecnai TF30 “Polara” Microscope (FEI, Eindhoven) operating at 300 keV. The microscope was equipped with a Gatan Imaging Filter “Quantum” energy filter operated in zero-loss mode with a 20 eV wide slit, and a post energy filter mounted K2 Summit direct electron detector (Gatan, Inc.) Data were acquired in counting mode, with aligned frames produced ‘on the fly’, using the combined filter for image alignment in Digital Micrograph (Gatan, Inc.). Dose, pixel size, magnification and tilt angle information are provided in Table S1. Data were acquired using SerialEM (Boulder, Colorado) (Mastronarde, 2005).

2.3. Tomogram reconstruction, segmentation and subvolume averaging

Tilt series outputted from the microscope were aligned and reconstructed using the IMOD software package (Kremer et al.,

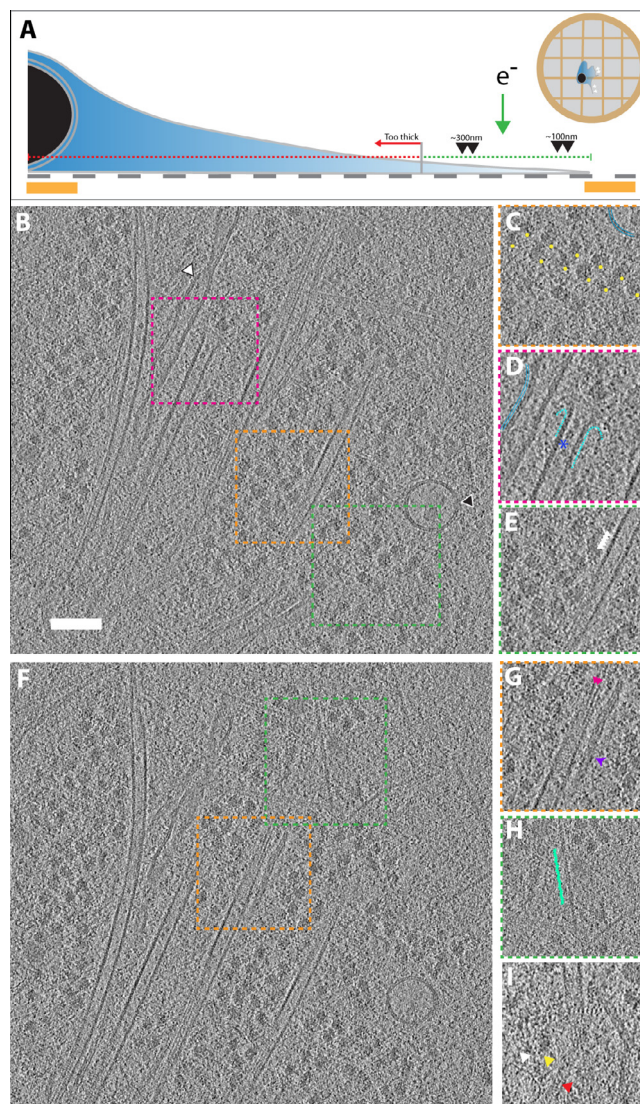


Fig. 1. CryoET of a peripheral region of an adherent U87MG neuronal cell line imaged using direct electron detection. (A) Schematic representation of an adherent cell grown on a holey carbon-coated gold grid. Red line indicates regions too thick for cryoET imaging. Area marked by green line indicates typical regions of the cell accessible to imaging by cryoET. (B) Slice through tomogram at the periphery of the U87MG cell, containing a number of cellular features such as (C) polysomes, (D) a de-polymerising microtubule in proximity to the endoplasmic reticulum with microtubule luminal bodies (blue asterisk), and (E) 4 nm tubulin spacing of the microtubule. White and black arrows in (B) represent the endoplasmic reticulum and a lysosome, respectively. (F) Another slice through the same tomogram, showing the diversity of cytoskeletal elements visible in a snapshot of the cell periphery; (G) microtubule protofilaments (pink arrows) (top-view), intermediate filaments (purple arrow) and (H) F-actin (green). (I) Vault ribonucleoprotein cage (white arrow) and a putative cytoskeletal motor, dynein (yellow arrow), engaged with a microtubule (red arrow), cf. also Fig. S2. Squares outlined by colored dashed lines in (B) and (F) indicate positions of areas in (C–E) and (G–H), respectively. Scale bar; 100 nm. Thickness of the tomographic slices is 4.22 Å for all panels.

1996). CTF correction, where applicable, was also performed using IMOD. A global defocus was determined for the whole tomogram, which was then used to correct individual tilts in the tilt series, taking into account the change in eucentricity across the projection images at high tilts. Phase flipping was then performed on each tilt image and the tomogram reconstructed using this phase flipped image stack. Sub-volume averaging of microtubules was performed using PEET (also part of IMOD) (Nicastro et al., 2006). Particles were picked from tomograms binned by a factor of 4, using scripts based on TEMPY (Farabella et al., 2015) that evenly sampled

Download English Version:

<https://daneshyari.com/en/article/5591556>

Download Persian Version:

<https://daneshyari.com/article/5591556>

[Daneshyari.com](https://daneshyari.com)